Journal of Fluorescence, Vol. 12, Nos. 3/4, December 2002 (© 2002)

Growth Behavior of CdS Nanoparticles Embedded in Polymer and Sol-Gel Silica Matrices: Relationship with Surface-State Related Luminescence

B. Bhattacharjee,[1] D. Ganguli,[1,2] and S. Chaudhuri[1]

Received May 21, 2002; revised July 22, 2002; accepted July 22, 2002

Chemical techniques were employed to synthesize CdS nanoparticles embedded in polymer (PEG 300) and sol-gel silica matrices. Systematic growth of particles (radius 3–9 nm) was obtained by adjusting post-deposition annealing temperature and time to examine the dependence of surface-state–related luminescence on particle size. Photoluminescence (PL) peak energy showed a linear dependence with a gentle slope in the weak confinement region and a steep slope in the strong confinement region, the divergence being observed near the excitonic Bohr radius for CdS. The empirical relation proposed for the weak confinement region could be used for estimating chemically prepared CdS nanoparticle size with a high degree of reliability from PL peak energy.

KEY WORDS: CdS nanoparticles; surface state related luminescence; particle growth.

INTRODUCTION

Semiconductor nanoparticles are characterized optically by, among other factors, their fluorescence spectra. Fluorescence in a semiconductor is determined by radiative transition compared to the nonradiative transitions occurring through various recombination centres or surface states. There are various types of surface states that give rise to different energy states inside the semiconductor band gap. Surface states due to dangling bonds are deep traps. In addition there may be vacancies because of nonstoichiometry, interstitial or substitutional impurities, and impurity vacancy complexes. With reduction of size of the nanocrystallites the surface to volume ratio is increased and there is a rapid increase of surface states, which often promotes nonradiative recombination.

Even if there is charge neutrality inside a nanoparticle, the surface of it may be charged because of presence of dangling bonds/defect states. Because of the high density of these defect states with decreasing particle size the recombination at the surface of the nanoparticle increases rapidly. So when an exciting radiation falls on such a nanoparticle there may be recombination at the surface without reaching inside, which may be detrimental for fluorescence. If the surface states extend up to a certain thickness (top layer) of the nanoparticle, making its surface charged, there will be a depletion layer of nearly the same width. The widths of the charged surface layer and depletion layer depend on the fabrication technique of the nanocrystalline semiconductor sample. If the nanoparticles are embedded inside a suitable matrix, the surface states may be passivated to some extent and the properties of the nanoparticle may be controllable, which is an essential requirement for device fabrication. There is some controversy about the dependence of fluorescence on surface states. Hence it needs further investigation so that a clear picture about the effect of surface states may emerge.

Systematic fluorescence studies on semiconductor nanoparticles by different groups [1–3] indicated that the characteristic luminescence is caused by excitonic

[1] Department of Materials Science, Indian Association for the Cultivation of Science, Kolkata 700 032, India.
[2] To whom correspondence should be addressed. e-mail: mssc2@iacs.res.in

1053-0509/02/1200-0369/0

recombination, in association with significant contributions from impurities and surface states in the lower-energy part of the photoluminescence (PL) spectra. With decreasing size of the nanocrystallites, the density of the surface states would increase as a result of increase in surface to volume ratio; as a consequence, the luminescence has often been found to be dominated by surface state transitions rather than excitonic transitions.

Band edge luminescence has been studied rigorously [4–7], and the line shape analysis was used to determine the average grain size, as well as size distribution. It has been well established that the excitonic luminescence is size dependent and the emission shifts to the blue region with decreasing particle size. Thus the band edge luminescence can be used as a tool to monitor the grain growth process. Recently, the aggregation of silica particles during hydrogel polymerization has been observed using the combined fluorescence anisotropy decay of solvated and bound dye [8].

Not many systematic reports have been found on the study of the size dependence of the surface-state–related luminescence. Some reports [9,10] indicated that luminescence from surface states does not vary much upon decreasing particle sizes. Chen *et al.* [11], on the other hand, observed that the surface emission shifts to the blue region as the size of the particles decreases for chemically prepared ZnS nanoparticles. This size dependence of the surface emission was in agreement with their optical absorption and thermoluminescence. Mandal *et al.* [12] observed similar size dependence of surface emission for ZnS nanocrystalline thin films prepared by high-pressure magnetron sputtering. The shift of the surface emission because of size variation has been reported and discussed by Chestnoy *et al.* [13]. Wada *et al.* [14] attributed the red shift of the surface emission not to the particle growth but to the changes in the surface structures for microwave-assisted growth of CdS nanocrystallites. Qi *et al.* [15] found that the emission from the surface state was related to the particle size and the PL emission blue shifted with decreasing particle size for CdS nanoparticles stabilized by double-hydrophilic block copolymers. None of the above reports attempted any type of direct and quantitative correlation for the size dependence of the trapped luminescence that can be used to monitor the grain growth using only the fluorescence spectroscopy, and thus there is no simple theoretical relationship between nanocrystalline size and peak emission wavelength.

In this communication, an attempt has been made to study the grain growth process of cadmium sulphide nanocrystals in two different hosts using the corresponding surface state luminescence spectra. The expectation of this work was to arrive at a possible qualitative correlation with a predictive value, that is, estimation of nanoparticle size from the surface state luminescence spectra.

EXPERIMENTAL

Preparation of CdS nanoparticles embedded in thin films of (a) a polyethylene glycol (PEG)-based solution and (b) an alkoxide-derived silica sol consisted of two steps: preparation of a solution or sol for the host material and that of a solution for the nanoparticles. Brief descriptions are given below.

In the process of preparation of a solution for deposition of the composite films of CdS nanoparticles dispersed in polymer matrix, polyethylene glycol (PEG 300, Merck, India) was dissolved in dry ethanol (dried over activated molecular sieve zeolite 4A under agitation). Glacial acetic acid (GR, Merck India) was added into the ethanolic solution under stirring, which was continued for ~1 hr. This part of the solution had the composition PEG 300:acetic acid:dry ethanol = 1.25:1:17.5 (molar ratio). For the preparation of the films of CdS nanoparticles embedded in silica matrix, a silica sol was first prepared by dissolution of tetraethyl orthosilicate, $Si(OC_2H_5)_4$ (TEOS, for synthesis, Merck.Schuchardt) in 2-propanol, $(CH_3)_2CHOH$ (GR, Merck India) dried over activated molecular sieve Zeolite 4A and addition of distilled water. Hydrochloric acid (0.1 N) (Titrisol, Merck India) was added as catalyst.

For synthesis of CdS in the above matrices, a solution suitable for both was separately prepared. $Cd(NO_3).4H_2O$ (Pure, Merck, India) and NH_2CSNH_2 (Purified, Merck, India) were used as the precursors for incorporation of Cd and S, respectively. These precursors were dissolved together in dry ethanol (for PEG solution) or dry 2-propanol (for silica) and distilled water under stirring. The precursor solutions of CdS were mixed carefully with the respective precursor solutions for the host to obtain clear and transparent solutions in both cases. The final solutions were stirred again for another 4–5 hr and aged overnight before preparing the films. Films were prepared by keeping the molar ratio of PEG 300 to CdS = 50:50 and equivalent SiO_2 to CdS = 70:30.

The composite films were deposited by spin coating (~3000 rpm) on properly cleaned soda-lime glass substrates (for optical measurements) and on C-coated Cu grid (for transmission electron microscopy). Post-deposition annealing treatment for the formation of CdS nanoparticles was carried out in the temperature range 373–473 K for 10–120 min. The films were characterized by measuring the optical transmittance and reflectance as a function of wavelength using a spectrophotometer

(Hitachi-U3410) in the wavelength region 350–800 nm. Transmission electron micrographs (TEM) were obtained using a Hitachi-H 600 unit. Photoluminescence (PL) spectra were recorded on a Perkin Elmer LS 55 luminescence spectrometer. The excitation source used was a xenon lamp.

RESULTS AND DISCUSSIONS

When the films were annealed at different temperatures for a fixed time period, or for different times at a fixed temperature, nucleation and growth of CdS nanoparticles occurred both in the polymer and sol-gel silica matrices. Figure 1 shows, as an example, representative TEM of the CdS nanoparticles embedded in PEG 300 matrix. Typical grain growth was observed with increasing annealing temperature or time. It also could be observed from the figures that, in all cases, the particles are nearly monosized and no significant size distribution occurred in the nanocrystals. Figure 2a shows the variation of the optical absorption coefficient (α) of the CdS nanocrystallites with photon energy ($h\nu$) dispersed in PEG (curves a–c) and sol-gel silica (curves d–g) matrices, respectively. The red shift of the fundamental absorption edge with increasing annealing temperature (T) and/or annealing time (t) was evident in the case of both the matrices indicating typical growth of the particles, their sizes increasing with heat treatment. In all cases, the optical band gaps obtained using these spectra were greater than the bulk band gap of CdS. This indicates that nano size of the particles was retained in our whole experimental range. The particle radii (r) were measured in all cases from the blue shift of the optical band gap because of the quantum confinement. Particle radii were also measured, whenever possible, from transmission electron micrographs (accuracy ± 0.5 nm) as support of the values obtained using optical spectra. Table I shows examples of the matching in the particle radii values obtained via two methods of measurement for different experimental conditions. Figure 2 shows the variation of average particle radii (r) with annealing time (t) (curves a and b) and annealing temperature (T) (curves c and d), respectively, for the series CdS:PEG = 50:50 and SiO_2:CdS = 70:30 (molar). Significant changes were observed in average particle radii (r) with increase in t or T. Figure 3 shows some representative PL spectra for CdS nanoparticles embedded in PEG (Fig. 3a) and silica matrices (Fig. 3b), respectively. PL spectra for the films with different particle sizes were recorded at room temperature with an excitation wavelength of 400 nm. In both cases the spectra were broad and emission occurred at lower energy values than those for the excitonic emission band. This could be attributed to the recombination

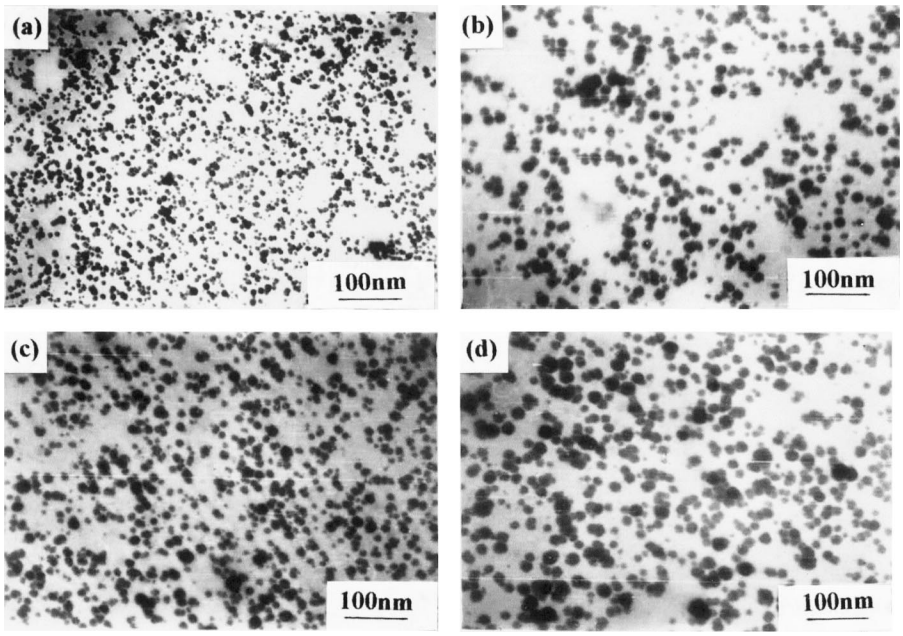

Fig. 1. Transmission electron micrographs of CdS nanoparticles in PEG matrix with PEG:CdS = 50:50 (molar) for (a) annealing temperature (T) = 373 K, annealing time (t) = 30 min; (b) T = 373 K, t = 120 min; (c) T = 413 K, t = 30 min; (d) T = 473 K, t = 30 min.

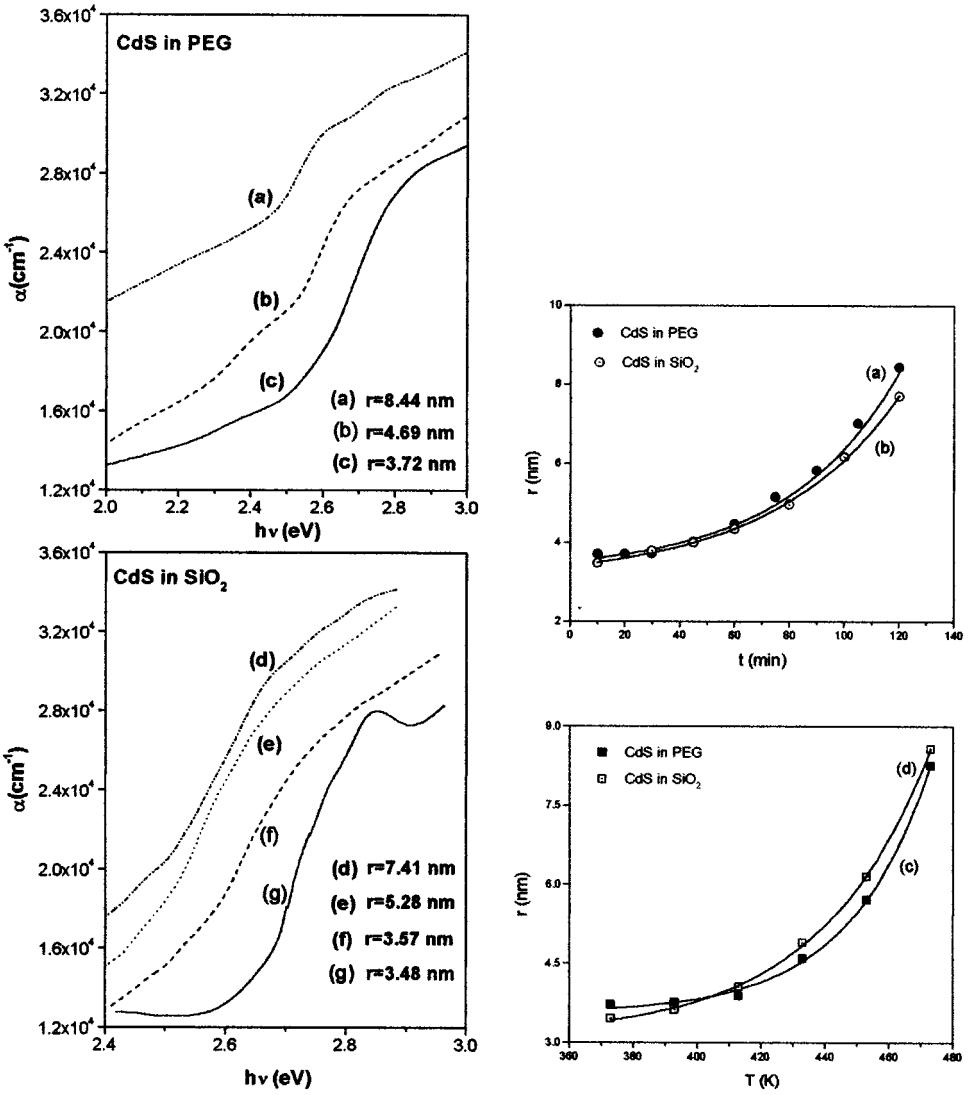

Fig. 2. (**A**) Optical absorption spectra of the CdS nanocrystallites dispersed in PEG (curves a to c): (a) T = 373 K, t = 120 min; (b) T = 373 K, t = 60 min; (c) T = 373 K, t = 30 min; and sol-gel silica (curves d to g) matrices: (d) T = 373 K, 120 min; (e) T = 433 K, t = 45 min; (f) T = 413 K, t = 30 min; and (g) T = 373 K, t = 30 min, with corresponding particle radii (*r*) obtained from these spectra. (**B**) Variation of average particle radii (*r*) with annealing time (*t*) for (a) CdS nanoparticles in PEG matrix; (b) CdS nanoparticles in sol-gel silica matrix; and variation of average particle radii (r) with annealing temperature (T) for (c) CdS nanoparticles in PEG matrix; and (d) CdS nanoparticles in sol-gel silica matrix. (The lines drawn in the figures are only for visual guidance.)

of the charge carriers trapped in the surface states [15]. It was clear from the figures that the PL emission peaks red shifted with increasing particle radii. When the PL emission energy was plotted against the growing particle radii as a function of increasing temperature or time in both the hosts, two different slopes were observed (Fig. 4). For relatively small particle sizes, the slope was very steep, whereas for larger particles, the slope was relatively gentle. The value of radius r_c, for which this change occurred, was determined from the divergence (Fig. 5) that occurred in the second derivative (d^2p/dr^2) of the slope of the curve (p) in Fig. 4. This value was determined as 3.7 nm, close to the excitonic Bohr radius of CdS (3.4 nm). For the particle sizes greater than this value, a general linear relationship was obtained. The relationship can be empirically expressed as

Table I. Average Particle Radii (r) for Nanocrystalline CdS Films Annealed at Different Conditions (Temperature = T and Time = t) with Molar Ratio of PEG:CdS = 50:50

Condition for film synthesis	r from blue shift of optical band gap (nm)	r from TEM (nm)
T = 373K, t = 30 min	3.72	3.60
T = 373K, t = 60 min	4.69	4.50
T = 373K, t = 90 min	5.82	5.90
T = 373K, t = 120 min	8.44	8.60
T = 413K, t = 30 min	3.86	4.00
T = 433K, t = 30 min	4.60	4.40
T = 473K, t = 30 min	8.26	8.40

$$E(r) = E_0 - kr \quad (1)$$

where E_0 is the theoretical extrapolated value of the PL emission energy at vanishingly small radius with slope *k*. In the present case, the slope is $0.0157 \pm 5 \times 10^{-4}$ (eV/nm) (inset, Fig. 5), indicating a clear dependence of PL peak energy on particle size in this weak confinement region; the intercept was estimated as $2.269 \pm 2.96 \times 10^{-2}$ eV. The value of the correlation coefficient in this case was -0.998, which showed that the reliability of the straight line fitting in the present case was very high. It may be noticed that this same equation represents the growth behavior of CdS particles as a function of increasing time or temperature in both PEG and silica matrices.

The relationship between R, the distance between two trapping sites (such as donor–acceptor pairs) and the emission wavelength of the defects in bulk II–IV semiconductor crystals was used by Chestnoy *et al.* [13] to explain the size dependence of the surface emission. The Coulomb potential $e^2/\varepsilon R$ was considered to be an important term determining the emission energy of the surface states, and it was pointed out that close pairs with small trapping distance emit at higher energy than distant pairs. This model is not able to explain the surface emission reasonably, because the distance between two trapped carriers has been considered not to be related to the size of the particles but to the density of the trapped carriers [11]. On the other hand, the size-dependent behavior of the surface-state–related PL peak energy can be explained by the model proposed by Chen *et al.* [11]. The trap depth does not change significantly upon decreasing the particle size, but the band gap increases as the size is decreased. Thus the energy separation between the charge carriers increases with decreasing size. As a result, the luminescence of the surface states shifts to the blue region as the size is decreased. As in the case of very fine particles, the blue shift in band gap

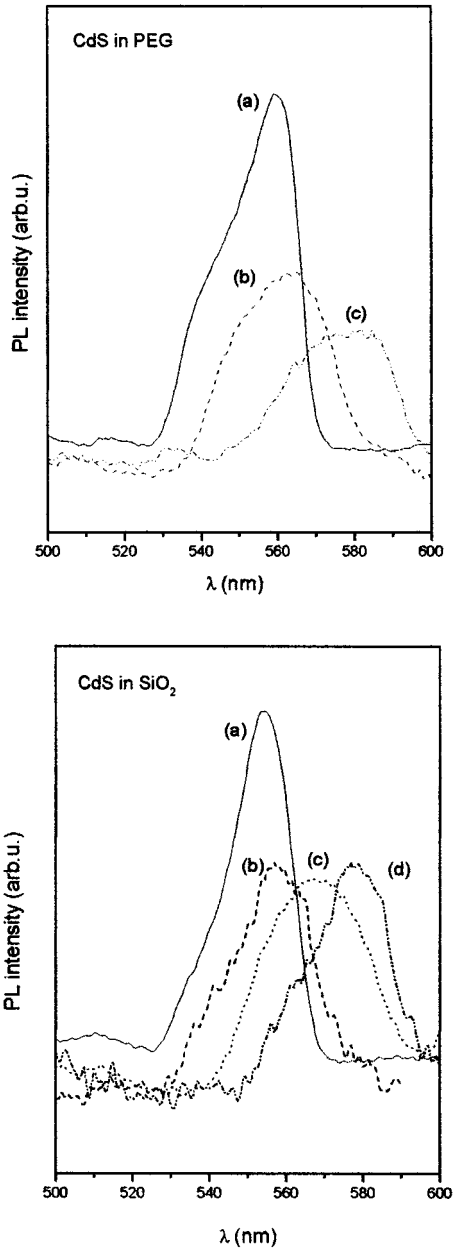

Fig. 3. (**A**) Photoluminescence (PL) spectra of representative CdS nanocrystallites embedded in PEG matrix (PEG:CdS = 50:50, molar): (a) T = 373 K, t = 30 min; *r* = 3.72 nm; (b) T = 373 K, t = 60 min; *r* = 4.69 nm; (c) T = 373 K, t = 120 min; r = 8.44 nm. (**B**) PL spectra of representative CdS nanocrystallites embedded in sol-gel silica matrix (SiO_2: CdS = 70:30, molar): (a) T = 373 K, 30 min, *r* = 3.48 nm; (b) T = 413 K, t = 30 min, r = 3.57 nm; (c) T = 433 K, t = 45 min, r = 5.28 nm; (d) T = 373 K, t = 120 min, *r* = 7.41 nm.

occurs at a faster rate; the PL emission energy accordingly should change with particle radii at a faster rate, making a steeper slope in the peak energy (E) vs. r curve. This

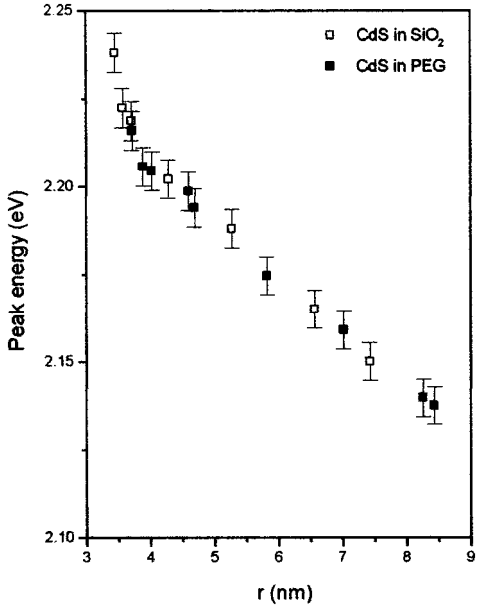

Fig. 4. Variation of PL peak energy (E) with average particle radii (r) for ■ CdS nanoparticles embedded in PEG matrix and □ CdS nanoparticles embedded in sol-gel silica matrix.

has been experimentally observed in our system for r $<$3.7 nm (Fig. 4). However, this agreement is qualitative; quantitative analysis needs inclusion of several factors (e.g., trap state density, ionization of defect, etc.) in the above model.

It can be noticed that the two host materials exerted similar (not necessarily the same) protective influence on the particle size. Thus all the points on the E vs. r curve (see Fig. 4) fell on a straight line with a very high correlation coefficient, indicating that no abnormal growth of the particles took place under any of the time or temperature conditions. This further shows that the empirical linear equation thus obtained has a significant predictive value for CdS nanoparticle size determination, and, thus, determination of particle growth rate as a function of surface-state–related luminescence. A similar relationship also has been obtained for ZnS nanoparticles in sol-gel silica matrix [16].

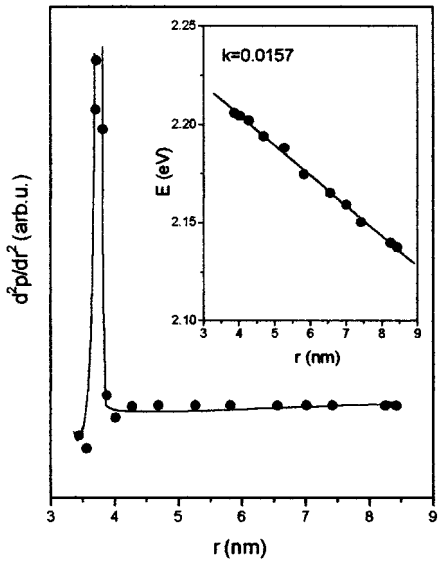

Fig. 5. Second derivative (d^2p/dr^2) of the slope of the curve (p) in Fig. 4 (inset) straight line fit to the variation of PL peak energy (E), with average particle radii (r) for the larger particle sizes.

CONCLUSIONS

Growth of CdS nanoparticles in polymer and sol-gel silica matrices was studied using the fluorescence arising from the surface states. PL emission energy showed a linear dependence on particle size above a certain value of radius close to the excitonic Bohr radius. The relationship as expressed in a linear equation had a high value of correlation coefficient (-0.998) and could probably be used for monitoring growth of chemically derived CdS nanoparticles over a large stretch of size and irrespective of their nature (organic, inorganic) of confinement.

REFERENCES

1. B. Andrianasolo, B. Champagnon, M. Ferrari, and N. Neurot (1991) Non-linear effects in microcrystalline semiconductors, *J. Luminesc* **48**, **49**, 306–308.
2. M. Danek, K. F. Jensen, C. B. Murray, and M. G. Bawendi (1994) Preparation of II-VI quantum dot composites by electrospray organometallic chemical vapor deposition, *J. Cryst. Growth* **145**, 714–720.
3. F. Hache, M. C. Klein, D. Ricard, and C. Flytzanis (1994) Photoluminescence study of Schott commercial and experimental CdSSe doped glasses: Observation of surface states, *J. Opt. Soc. Am. B* **8**, 1802–1806.
4. K. Kohno, Y. Osaka, F. Toyomura, and H. Katayama (1994) Photoluminescence of Si microcrystals embedded in SiO_2 glass films, *Jpn. J. Appl. Phys.* **33**, 6616–6622.
5. Y. Osaka, K. Tsunetomo, F. Toyomura, H. Myorer, and K. Kohno (1992) Visible photoluminescence from Si microcrystals embedded in SiO_2 glass films, *Jpn. J. Appl. Phys. B* **31**, L365–L366.
6. Y. Ohfuti and K. Cho (1996) Size and shape dependent optical properties of assembled semiconductor spheres, *J. Luminesc* **70**, 203–211.
7. M. C. Klein, F. Hache, D. Ricard, and C. Flytzanis (1990) Size dependence of electron-phonon coupling in semiconductor nanospheres: The case of CdSe. *Phys. Rev. B* **42**, 11 123–11 132.
8. D. J. S. Birch and C. D. Geddes (2000) Sol-gel particle growth studied using fluorescence anisotropy: An alternative to scattering techniques, *Phys. Rev. E* **62**, 2977–2980.
9. M. Agata, H. Kurase, S. Hayashi, and K. Yamamoto (1990) Photoluminescence spectra of gas-evaporated CdS microcrystals. *Solid State Commun.* **76**, 1061–1065.

10. T. Arai, T. Yoshida, and T. Ogawa (1987) Photoacoustic and luminescence spectra of CdS fine particles, *Jpn. J. Appl. Phys.* **26**, 396–404.
11. W. Chen, Z. Wang, Z. Lin, and L. Lin (1997) Absorption and luminescence of the surface states in ZnS nanoparticles, *J. Appl. Phys.* **82**, 3111–3115.
12. S. K. Mandal, S. Chaudhuri, and A. K. Pal (1999) Optical properties of nanocrystalline ZnS films prepared by high pressure magnetron sputtering, *Thin Solid Films* **350**, 209–213.
13. N. Chestnoy, T. D. Harris, R. Hull, and L. E. Brus (1986) Luminescence and photophysics of CdS semiconductor clusters: The nature of the emitting electronic state. *J. Phys. Chem.* **90**, 3393–3399.
14. Y. Wada, H. Kuramoto, J. Anand, T. Kitamura, T. Sakata, H. Mori, and S. Yanagida (2001) *J. Mater. Chem.* **11**, 1936–1940.
15. L. Qi, H. Cölfen, and M. Antonietti (2001) Synthesis and characterization of CdS nanoparticles stabilized by double-hydrophilic block copolymers. *Nanoletters* **1**, 61–65.
16. B. Bhattacharjee, D. Ganguli, and S. Chaudhuri (2002) Surface state related luminescence of ZnS nanoparticles embedded in sol-gel silica matrix. (to be communicated).